Supplementary Information

Confined Tandem Catalytic Quasi-Solid Sulfur Reversible Conversion for All-Solid-State Na-S Batteries

Weiwei Zhang[a,b,1], Bin Song[c,1], Mingli Wang[a,d], Tingting Miao[e], Xiang-Long Huang[f], Erhuan Zhang[g], Xiaowen Zhan[a], Yue Yang[h], Hong Zhang[d,*], and Ke Lu[a,*]

[a]Institutes of Physical Science and Information Technology, School of Materials Science and Engineering, Anhui University, Hefei, Anhui 230601, China. *Email: luke@ahu.edu.cn (K.L.)
[b]School of Chemistry and Chemical Engineering, Qufu Normal University, Qufu, Shandong 273165, China.
[c]Institute of Functional Nano & Soft Materials (FUNSOM), Soochow University, Suzhou, Jiangsu 215123, China.
[d]School of Chemistry and Chemical Engineering, Harbin Institute of Technology, Harbin, Heilongjiang 150001, China. *Email: zhanghonghit@hit.edu.cn (H.Z.)
[e]Institute of Health and Elderly Care, Shandong Institute of Commerce and Technology, Jinan, Shandong 250103, China.
[f]Institute of Energy Materials Science, University of Shanghai for Science and Technology, Shanghai 200093, China.
[g]Global Institute of Future Technology, Shanghai Jiao Tong University, Shanghai 200240, China.
[h]School of Minerals Processing and Bioengineering, Central South University, Changsha, Hunan 410083, China.
[1]W.Z. and B.S. contributed equally to this work.

Sample preparation

Preparation of the MnO₂ nanowire: In a typical process, 2.0289 g of $MnSO_4 \cdot H_2O$ (Adamas) and 8 mL 0.5 M H_2SO_4 (Adamas) were added into 300 mL deionized (DI) water as solution A. 1.264 g of $KMnO_4$ (Adamas) was dissolved in 100 mL of DI water as solution B. Solution B was slowly added to the solution A under stirring and stirred for 2 h. Then, the mixture was transferred to a Teflon-lined autoclave and heated at 120 °C for 2h. The resultant precipitation was washed with DI water and ethanol and then vacuum dried, which was named MnO_2 nanowire.

Preparation of the MnHCF/PPy@MnO₂: First, 0.3 g of MnO_2 nanowire was added into 100 mL DI water. 0.4 g of $K_3Fe(CN)_6 \cdot 3H_2O$ (Adamas), 200 μL pyrrole (Adamas), and 2mL 0.5 M HCl (Adamas) were added into the 50 mL ethanol (Adamas) and water (v:v = 1:1) solution. After that, the pyrrole solution was added to the MnO_2-containing solution dropwise under stirring for 4h. The solution was then treated by centrifugation to obtain the core-shell structured polymer@MnO₂ products, which were then washed with ethanol and vacuum-dried. The Mn^{4+}/Mn^{2+} redox couple ($MnO_2 + 4H^+ + 2e^- \rightarrow Mn^{2+} + 2H_2O$ (1.23 V vs. RHE)) has higher redox potential than polymerization potential of monomers ($nC_4H_4NH \rightarrow (C_4H_2NH)_n + 2nH^+ + 2ne^-$ (~0.7 V vs. RHE)), the MnO_2 was employed as both sacrificial template and oxidation initiator to trigger the spontaneously interfacial polymerization of pyrrole, generating coaxial crosslinked polyaniline@MnO₂ (PPy@MnO₂) nanostructure with uniform polymer wrapping shells. Then, 100 mg of MnO_2@polymer was added into 100 mL 1M HCl solution with stirring and kept for 1 h for leaching out redundant metal oxide, which could generate the space between polymer and MnO_2 for hosting active sulfur species, the corresponding sample was marked as coaxial MnHCF/PPy@MnO₂. MnO₂@PPy was prepared through the same procedure, just replacing the $K_3Fe(CN)_6 \cdot 3H_2O$ with ammonium persulfate (APS, Adamas). Furthermore, the MnHCF/PPy nanotube was prepared by complete removal of metal oxides from MnHCF/PPy@MnO₂ during acid leaching. The PPy nanotube was obtained from the same process just replacing the PPy@MnO₂ with the MnHCF/PPy@MnO₂.

Preparation of the MnHCF/PPy@S@MnO₂: To load sulfur, the prepared MnHCF/PPy@MnO₂ matrix was thoroughly mixed with sulfur powder using a mortar and pestle in a mass ratio of 1:3. Then, the mixture was heated at 155 °C for 6 h in an Ar-filled autoclave to generate MnHCF/PPy@S@MnO₂ composite. Similarly, the control cathodes (PPy@S, MnHCF/PPy@S, and PPy@S@MnO₂) were obtained by the same process except that the MnHCF/PPy@MnO₂ was replaced by the corresponding matrix.

Sample characterization

The morphologies of samples were explored by using scanning electron microscopy (SEM, Hitachi 650 electron microscope) and transmission electron microscopy (TEM, JEM-2100F), equipped with energy dispersive spectroscopy (EDS, Bruker detector). The phase information of samples was obtained by using a Rigaku Miniflex diffractometer (Rigaku Corporation, Japan). The surface chemistry compositions of samples were detected by an X-ray photoelectron spectroscopy (XPS, ESCALAB 250). N_2 adsorption-desorption isotherms were measured at 77 K using a TriStar 3000 analyzer and 3Flex 3500. Prior to subsequent measurements, the sulfur-loaded composite materials were firstly dried at 110 °C for 10 h to remove the surface adsorbed sulfur and water. Then, the samples were degassed at 95 °C for 6 h.The specific surface areas and pore size distributions were calculated by the Brunauere-Emmete-Teller (BET) and the Barrett, Joyner, and Halenda (BJH) methods. The sulfur content of the MnHCF/PPy@S@MnO₂ composite was determined by thermal gravimetric analysis (TGA) (TG/DTA6300) under Ar flow and a ramp rate of 10 °C min⁻¹. Raman spectra were tested on a LabRAM HR 800 system with a 532 nm excitation laser. UV-vis absorbance spectra were measured using a Shimadzu UV-1800 spectrophotometer.

Electrochemical characterization

Beaker cell assemble and measurement: To fabricate the positive electrodes that work in flooded Na-S cells, Cathodes were prepared by casting of N-methyl pyrrolidone (NMP) slurry containing 85 wt % active materials (PPy@S, PPy@S@MnO₂, MnHCF/PPy@S, and MnHCF/PPy@S@MnO₂), 5 wt % CNT and 10 wt % binder polyvinylidene fluoride (PVDF). Then, the slurry is uniformly coated on the carbon paper and then dried in an argon-filled glove box for about 5 days to remove water/solvent. The electrodes were cut into discs of 12 mm and used directly. The mass loading of each electrode was in the range of 1.5-2.5 mg cm⁻². The electrolyte was 1M sodium bis(fluorosulfonyl)imide (NaFSI) dissolved in tetraethylene glycol dimethyl ether with a 1 wt% NaNO₃ additive. The galvanostatic charge-discharge was carried out by a

Neware BTS-4000 battery analyzer in a constant temperature chamber (25°C). Capacities are calculated based on the mass of sulfur. The beaker cells were assembled by using the PPy@S, PPy@S@MnO$_2$, MnHCF/PPy@S, and MnHCF/PPy@S@MnO$_2$ electrodes as cathodes and Na metal foil as the anode. The sulfur loading of all positive electrodes was 1.2 mg cm^{-2} and the active area immersed in electrolyte was about 1 cm^2. After 50 cycles, the electrolyte was tested by UV-vis spectrometer to compare the residual polysulfide concentrations.

Solid-state Na-S cells: The working electrode that operated in the solid-state Na-S cell was prepared by mixing 85 wt% MnHCF/PPy@S@MnO$_2$ composite powder, 10 wt% PEO$_{10}$-NaFSI binder, and 5 wt% CNT additive in acetonitrile under the dry atmosphere to form a cathode slurry. After that, the mixture was cast on a clean Teflon plate and further dried in an Ar-filled glove box for about 5 days to remove the solvent. The active material loading within the cathode film was around 1.0-2.0 mg cm^{-2}. All cyclic voltammetry (CV) was performed on a CHI 660E electrochemical workstation. Batteries were cycled at 80 °C with a voltage of 1.0~2.5 V using a battery analyzer (Neware BTS-4000 battery analyzer) at desired current densities.

In situ analyses: The in situ Raman spectra were obtained with a Lab Renishaw InVia Raman spectrometer with 532 nm laser excitation. It was performed on Gamry Reference 600 electrochemical workstation with galvanostatic charge-discharge measurements at 10 mA g^{-1} and 1.0-2.5 V vs Na. In situ XRD measurement was collected on Multifunctional X-ray diffractometer (XRD, Rigaku Co, Japan, D/MAX-γA) for the first cycle at 2θ values ranging from 10° to 24° with a scanning rate of 1° min^{-1} and 1.0-2.5 V vs Na. During in situ XRD process, the cathode was prepared by mixing 90 wt% MnHCF/PPy@S@MnO$_2$ composite powder and 10 wt% PEO$_{10}$-NaFSI binder with the sulfur loading was about 2 mg cm^{-2} and the charging/discharging currentdensity was set to 2 mA g^{-1}. Transparent cells for in situ UV-Vis spectra were assembled on standard glass slides. The sulfur cathode was prepared by mixing 80 wt% MnHCF/PPy@S@MnO$_2$, 10 wt% conductive carbon, and 10 wt% PVDF with the sulfur loading was about 1.5 mg cm^{-2}. Na metal foil was employed as anode and the cell with the addition of 3 mL 1M NaFSI electrolyte was assembled in the argon-filled glove boxe and then galvanostatically tested at 1 mA cm^{-2}.

DFT calculation

All DFT calculations in this study were performed within Vienna Ab-inito Simulation Package (VASP). The Perdew-Burke-Ernzerhof functional within the generalized gradient approximation scheme was used for exchange-correlation calculation. Next, the core-valence interactions were evaluated by the projected augmented wave code. all process was involved by spin polarization. The 3×3×1 Monkhorst-Pack grid k-points were used to obtain the Brillouin zone integration. The energy cutoff for plane wave expansions was selected as 400 eV. The vacuum spacing in a direction perpendicular to the plane of the structure is 20 Å for the surfaces. The electronic energy was considered self-consistent when the energy change was smaller than 10^{-5} eV. A geometry optimization was considered convergent when the energy change was smaller than 0.05 eV Å^{-1}. Finally, all adsorption energies (E$_{ads}$) were calculated by the equation: $E_{ads} = E_{ad/sub} - E_{ad} - E_{sub}$, where Ead/sub, Ead, and Esub represent the total energies of the optimized adsorbate/substrate system, the adsorbate in the structure, and the clean substrate, respectively.
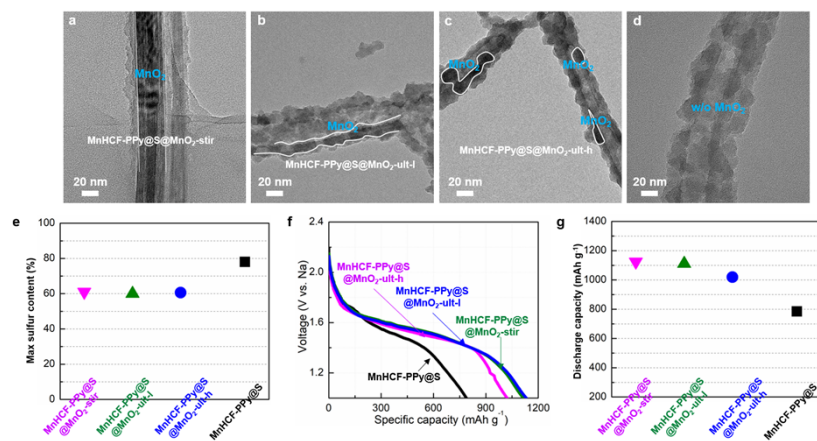
Figure S1. (a) TEM images of MnHCF/PPy@MnO$_2$ matrix after acid leaching 1 hour (continuously stirred at 300 rpm min^{-1}) of MnHCF/PPy@MnO$_2$ core-shell structured composites at 1 M HCl solution (100 mg powder/100 mL acid solution). TEM images of MnHCF/PPy@MnO$_2$ matrix after acid leaching of MnHCF/PPy@MnO$_2$ core-shell structured composites at 1 M HCl solution (100 mg powder/100 mL acid solution) under (b) low energy ultrasonic treatment for 5 min and high energy ultrasonic treatment for (c) 5 min and (d) 15 min. (e) Maximum sulfur uptake capability of different matrixes. (f) Comparision of discharge profiles of different sulfur cathodes as noted with the same sulfur mass loading (60 wt%) at 10 mA g^{-1} and 80 °C. (g) Specific discharge capacities of different cathodes between with the same sulfur loading at 60 wt%.
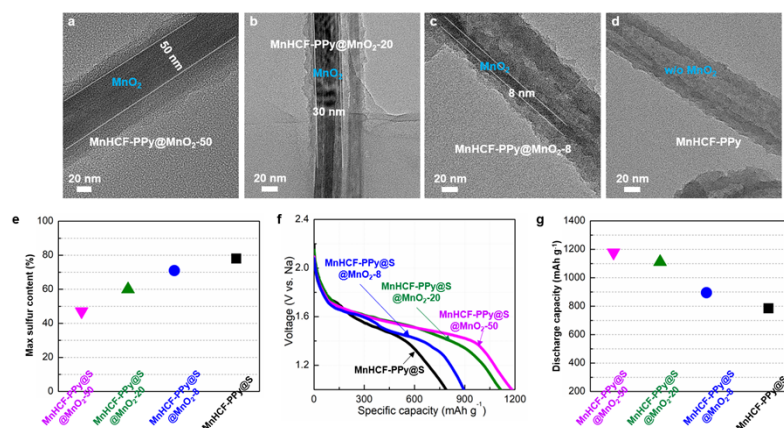

Figure S2. (a-d) TEM images of different MnHCF/PPy@MnO$_2$-based matrixes after acid leaching 0.3, 1, 2, 4 hour (continuously stirred at 300 rpm min^{-1}) of MnHCF/PPy@MnO$_2$ core-shell structured composites at 1 M HCl solution (100 mg powder/100 mL acid solution). (e) Maximum sulfur uptake capability of different matrixes. (f) Comparision of discharge profiles of different sulfur cathodes as noted with the same sulfur mass loading (60 wt%) at 10 mA g^{-1} and 80 °C. (g) Specific discharge capacities of different cathodes between with the same sulfur loading at 60 wt%.
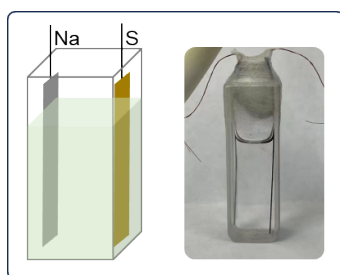
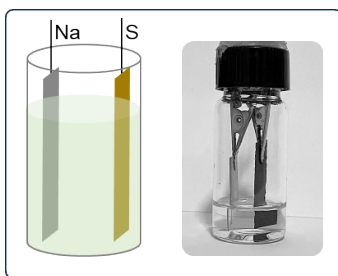**Figure S3.** Schematic image of the quartz cell for in-situ UV-Vis measurement.

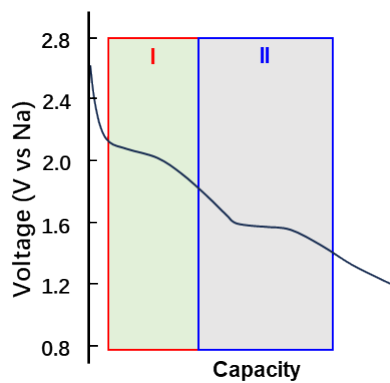**Figure S4.** Schematic of the Na-S beaker cell.

Figure S5. The discharge profile of Na-S batteries could be generalized into two main sequential stages.
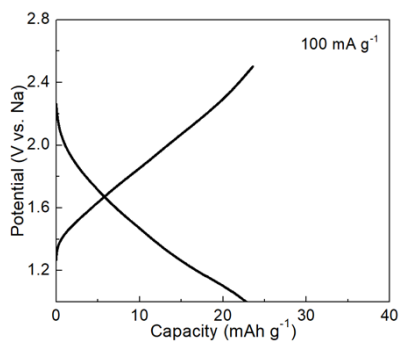

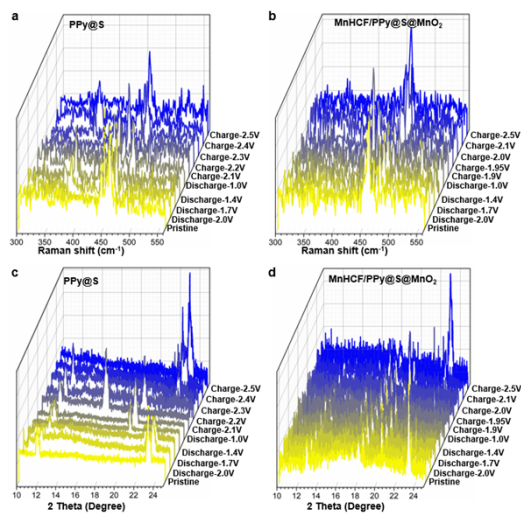**Figure S6.** Galvanostatic charge-discharge profiles of MnHCF/PPy@MnO$_2$ without loading sulfur.

Figure S7. The operando (a, b) Raman and (c, d) XRD patterns of typical selected sulfur cathodes during the initial discharge and charge processes.
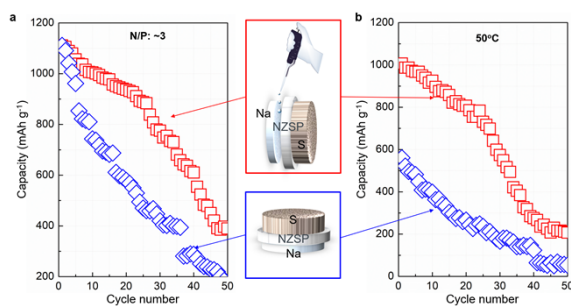

Figure S8. Cycle performance of different Na-S batteries at (a) the N/P ratio of ~3 and (b) 50 °C.